RESEARCHERID
THOMSON REUTERS

[FRTSSDS- June 2018]
DOI: 10.5281/zenodo.1302286

ISSN 2348 – 8034
Impact Factor- 5.070

GLOBAL JOURNAL OF ENGINEERING SCIENCE AND RESEARCHES

STRUCTURAL AND OPTICAL PROPERTIES OF NiFe2O4 VIA GREEN SYNTHESIS

S. Patel, P. Saxena & Dinesh Varshney*
School of Physics, VigyanBhavan, Devi Ahilya University, Indore, India

ABSTRACT

The nanoparticles of $NiFe_2O_4$ were successfully synthesized via green synthesis using banana peel extract as the catalyst as well as the medium for reaction technique is reported. Analysis of X-ray diffraction spectrum revealed the cubic spinel structure with the space group *Fd3m*. The Rietveld refinement was carried out which obeyed the results obtained from the XRD spectrum analysis of the sample. Raman spectrum provided confirmation for the spinel structure formation and five vibrations active Raman modes were observed. Since the optical band-gap value shows an inverse response to the crystallite size. The UV-Vis spectrum study confirmed dual but reduced band-gap value.

Keywords: Ferrites, Retvield refinement, Raman spectra, Band-gap
PACS: 7**5.85.+t, 61.05.cp, 78.30.−j;**.

I. INTRODUCTION

The research in nano-science may be aimed to explore, synthesis and understand new nanomaterials and the related phenomena. Magnetic nano-materials have gained great interests in the past few years for their fascinating applications. Recently nanocrystalline magnetic ferrite has received great attention due to their wide range of technological applications in various fields; such as magnetic fluids for storage of information's, ferrofluids, magnetically guided drug delivery, sensors, catalyst and magnetic resonance imaging (MRI) enhancement **[1-3]**. Among these, spinel ferrite, inverse ferrites are particularly interesting due to its high magnetocrystalline anisotropy, high saturation magnetization from typical crystal and magnetic structure **[4]**. Nano-crystalline ferrites which possesses a general formula MFe_2O_4 (M = divalent metal ion, e.g. Ni, Co, Cu, Mn, Mg, Zn, Cd, etc.) is one of the most attractive classes of materials for technological applications. In the present study, we investigate the synthesis of the nanocrystalline $NiFe_2O_4$ powders by green synthesis, followed by annealing the powders at moderate temperatures (800^0 C).

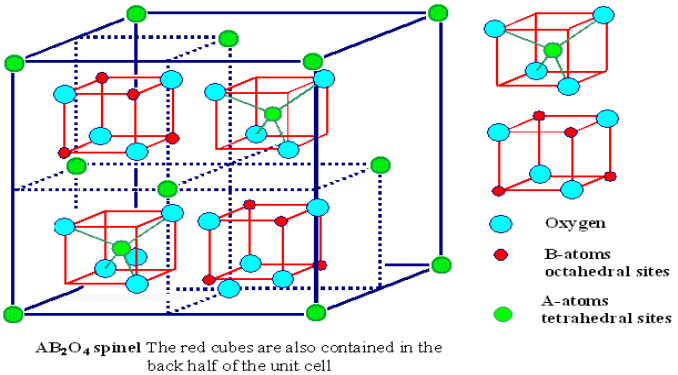

Fig. 1: Unit cell of structure of spinel ferrite.

Nickel ferrite ($NiFe_2O_4$) unit cell contains 32 oxygen atoms in cubic close packing with eight tetrahedral (A) and sixteen octahedral (B) sites. Half of the ferric ions preferentially fill the A-site and the others occupy the B-sites.

Thus, the compound can be represented by the formula: $(Fe^{3+})_A [Ni^{2+} Fe^{3+}]_B O_4^{2-}$ [5]. However, it shows ferrimagnetism that originates from magnetic moment of antiparallel spins between Fe^{3+} ions at tetrahedral sites and Ni^{2+} ions at octahedral sites shown in **Fig. 1**. In inverse spinel nickel ferrite nanoparticles, Fe^{3+} ions occupy *A* site fully while *B* site is occupied by Ni^{2+} and Fe^{3+} ions. It is thus the ferrimagnetism comes into existence in these materials of anti-parallel spins between Fe^{3+} and Ni^{2+} corresponding to *A* and *B* sites respectively. Many physical and chemical methods have been used to synthesize nanosize ferrites. The physical properties of ferrites depend on their composition, microstructure, the preparation method and the conditions for synthesis **[7-9].** Among these methods, mechanical milling, co-precipitation, hydrothermal reaction, micro emulsion method, and sol-gel techniques are commonly known. In a true sense, around the surface of the particle, reducing the particle size of a material modifies the physical properties. Nickel ferritenano particles exhibit ferrimagnetism or super-paramagnetism depending on the microstructure. Usually, ferrimagnetism is associated with samples with a grain size of 15 nm or more and super-paramagnetism occurs in samples of smaller grain size (<10 nm) **[4-6].**

Furthermore, the optical properties ofnano ferrites need to be explored. The optical response is indeed relevant from the technological point of view. The main objective of this work is tostudy the structural, optical and vibrationalproperties of nickel ferrite nanoparticles as prepared via green technology, a method totally different from the above conventional methods.

II. EXPERIMENTAL DETAILS

The banana peel washed distilled water and cut small pieces, 2 days on sunlight to dry the banana peel after put furnace for 2 hours a heating at 60°C. The dried peels were ground for 2 hours using mortar and pestle to get the fine powder. The weighed amount was mixed in 100 ml of distilled water in a beaker. The mixture was put on a magnetic stirrer for 1.5 hours with 450 rpm at room temperature. The mixture was then filtered to separate the precipitate. The stoichiometric amounts of the Ni $(NO_3)_2.6H_2O$ and $Fe(NO_3)_3.9H_2O$ were dissolved in the liquid extract at 60 °C with 550 rpm for 3h and later to remove the fluidity, the temperature was raised to 120 °C to get powder form of the sample. The sample was ground for 1h to get a fine powder and the remnant was put in a furnace at a calcination temperature of 800 °C for 6h and reground to have a fine powder of the sample.

The crystal structure and types of phases were identified by means of X-ray diffraction (XRD) at room temperature usi ng $CuK\alpha_1$ (0.15406 nm) radiation from a Bruker *D8* Advance X-ray diffractometer with a step size of 0.02^0 in the range of 2θ (20^0- 80^0). The data was collected with a step size of 0.02° over the angular range 2θ (20° < 2θ < 80°) generating X-ray by 40 kV and 40 mA power settings.

The Raman measurements were carried out using LABRAM - HR800 spectrometer equipped with a 50 × objective and a Peltier-cooled charge coupled device detector. The spectra were excited with 488 nm radiations (2.53 eV) from an air-cooled Argon Laser. UV-Vis spectrometer (Perkin Elmer, Lambda 950 - USA) was used to find the band gap of the sample under investigation.

III. RESULTS AND DISCUSSION

The x-ray diffraction pattern (XRD) of the bulk $NiFe_2O_4$ nanoparticles were prepared by low-temperature green synthesis route where the banana peel extract has used a solvent for precursors as well as a catalyst for the reaction to occur. The structure of prepared sample was examined by XRD characterization. **Fig 2 (a)** represents the diffraction pattern confirms the spinel phase, crystalline and nano-natured.

XRD patterns were analyzed to obtain the lattice parameter, using the expression $\mathbf{a= d\sqrt{h^2+k^2+l^2}}$, where ***a*** is lattice parameter, ***d***is inter-planner spacing and *(h, k, l)* are Miller indices. Obtained lattice parameter (***a***) was used to calculate the X-ray density of the sample using the following relation $\boldsymbol{\rho_{XRD} = (8M_w/Na^3)}$ where $\boldsymbol{\rho_{XRD}}$is X-ray density, $\boldsymbol{M_w}$is Molecular weight, ***N***is Avogadro's Number and **a** is lattice parameter. The crystallite size was calculated using Scherer formula: $D = k\lambda/\beta\cos\theta$, here '*D*' is crystallite size, λ is the wavelength of x-ray used (1.5406 Å), *k* is a constant (shape factor ≈ 0.9), θ is the angle of diffraction and β is the FWHM **[10].**

[FRTSSDS- June 2018]
DOI: 10.5281/zenodo.1302286

ISSN 2348 – 8034
Impact Factor- 5.070

The average crystallite size was found to be equal to 39 nm. The analysis of the XRD data further indicates that the prepared sample crystallizes into a cubic structure with the space group *Fd*-3*m*. High crystallinity and nano-size of the sample is evident from the intensity of the characteristic diffraction peaks and a broad FWHM **[6, 7].** Further, Rietveld refinement was carried out using FULLPROF software **[11]** represented by the**Fig 2 (b)** which confirmed the cubic structure, space group *Fd*-3*m* and the crystal structure concerned other parameters are shown in **Table: 1**

Table: 1 Observed XRD and Rietveld refined parameters of $NiFe_2O_4$.

Parameters	**Values**
Space Group	*Fd-3m*
a (Å)	8.34
V (Å^3)	580.35
Density (g/cm^3)	2.48
R_F	0.85
R_{Bragg}	0.99
R_{wp}	53.4
R_{exp}	41.2
R_p	115
□^{2}	1.68
GOF	1.3

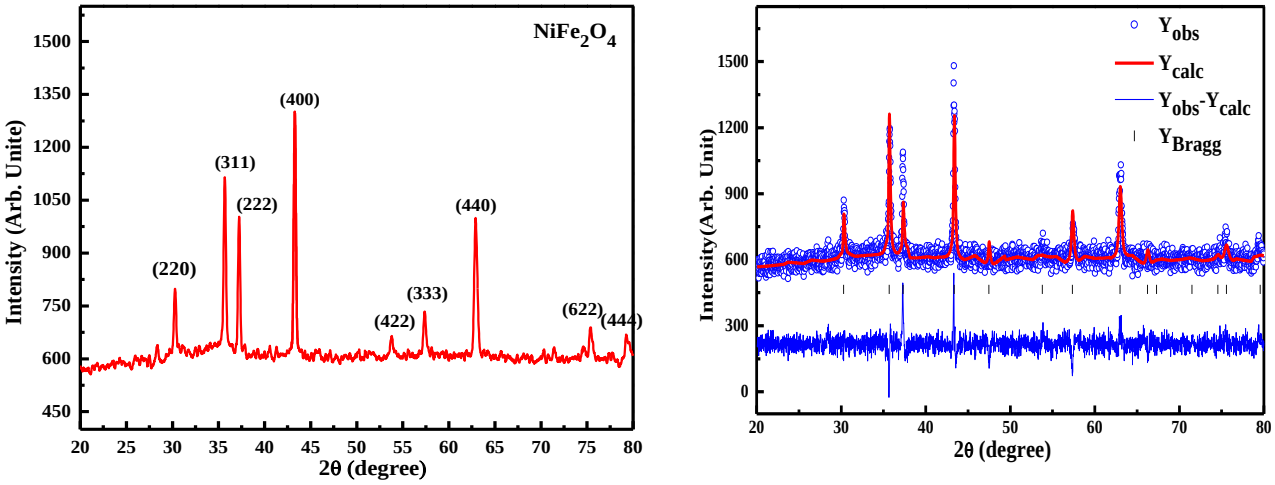

Fig. 2 (a).XRD spectrum of $NiFe_2O_4$ sample (b)Retvield refinement of $NiFe_2O_4$ sample.

$NiFe_2O_4$ has the space group *Fd-3m*(O_7^u). In this structure ,half of the Fe^{3+} cations are located on tetrahedral A-site whereas the rest of Fe^{3+} and Ni^{2+} cations are distributed over the octahedral B-site. According to the space group symmetry and factor group analysis, five Raman active internal modes such as A_{1g}, E_g, $T_{2g}(3)$, $T_{2g}(2)$, $T_{2g}(1)$, and E_g models are shown in **Table 2**. The modes from tetrahedral and octahedral sites can be distinguished by Raman spectroscopy. Raman peaks over the region of 660-20 cm^{-1} represent the tetrahedral modes in the ferrites, whereas the 460-40 cm^{-1} corresponds to the modes of the octahedral sites **[12-14].**

Fig. 3 shows Raman spectrum of $NiFe_2O_4$nano wires. The peaks at 336 cm^{-1} and 666 cm^{-1} shoulder with an average diameter of about 8 nm.Where A_{1g} mode symmetric stretching of oxygen atoms about Fe–O and Ni–O bonds in the tetrahedral sites and the E_g mode occurs due to symmetric bending of an oxygen atom with reference to the metal ion. The remaining $T_{2g}(2)$ and $T_{2g}(3)$ modes belong to the vibrations of the octahedral group. The $T_{2g}(3)$ mode is

believed to be due to the asymmetric bending oxygen and asymmetric stretching of Fe/Ni–O leading to $T_{2g}(2)$ mode. The $T_{2g}(1)$ mode is attributed to the translational movement of the tetrahedron. Raman modes in the region 660–720 cm^{-1} represent tetrahedral site in ferrites whereas modes in the region 460-640 cm^{-1} reveal the nature of the octahedral site.

Table:2 Observed Raman mode of $NiFe_2O_4$

Raman Modes(cm^{-1})	Ref.[12]	Observed
A_{1g}	705	702
E_g	655	663
$T_{2g}(3)$	540	576
$T_{2g}(2)$	488	485
$T_{2g}(1)$	334	331
E_g	230	214

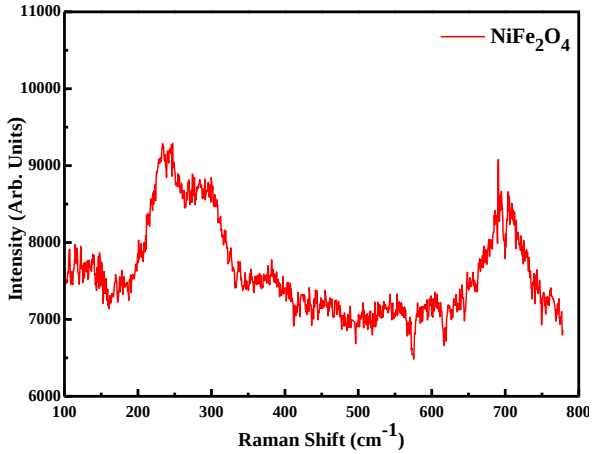

Fig.3.Raman spectrum of $NiFe_2O_4$ sample.

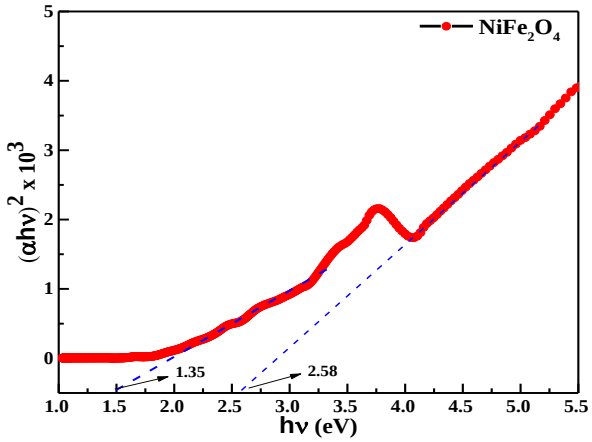

Fig. 4.Uv-Vis Spectrum for $NiFe_2O_4$.

The optical band gap *Eg* was estimated by plotting the square of the Kubelka-Munk function $(F(R)\ E)^{1/2}$ versus E(eV) graphs. The band gap (E_g) is studied by UV-Vis diffuse reflectance spectroscopy under the influence of preparation process, crystallite size. The following equation is employed to estimate the absorption band gap energy (E_g): $(\alpha h\nu)^n = k(h\nu - E_g)$, where, α is the absorption coefficient, $h\nu$ is the photon energy, k is the constant relative to the material, and n is either 2 for direct transition or 1/2 for an indirect transition **[15]**. The optical band gap energy of the sample is determined by using Tauc plots, $(ah\nu)^2$ vs. hν, as shown in **Fig. 4**. The extrapolation of the straight line segment to $(\alpha h\nu)^2 = 0$ gives two absorption band gap energies at 1.35 and 2.58 eV for $NiFe_2O_4$. No linear relation was found for n =1/2 which infers that the resulting sample exhibits directly allowed transitions. Since band gap energy is inversely related to the crystallite size, we got the lower value of band gap as the crystallite size is usually higher ≈ 40 nm. The observed band gap energies are due to the electronic transitions occurring from the O-2p valence band to the transition metals-3d (t_{2g}, e_g) conduction band. The two band gap energies of $NiFe_2O_4$ may be due to the co-existence of high spin and low spin sates in the $NiFe_2O_4$**[16, 17].**

IV. CONCLUSION

Nanocrystalline samples of $NiFe_2O_4$ ferrite were synthesized successfully using green technology. X-ray diffraction confirms single phased cubic (*Fd3m*) structure. The Rietveld refinement witnessed the results of the XRD spectrum. Raman spectrum analysis confirmed the spinel structure and displayed five Raman modes where additional modes

were observed. UV-Vis spectroscopy confirmed the dual band-gap nature, which is reduced due to the higher crystallite size when compared to the earlier reports.

V. ACKNOWLEDGMENT

UGC-DAE-CSR, as an institute is acknowledged for extending its facilities. Authors acknowledge Dr. V. Ganesan, Dr. M. Gupta, Dr. V. G. Sathe, Dr. U. Deshpande, and Mr. V. Ahire of UGC-DAE CSR, Indore for fruitful discussions. Financial support from UGC-DAE CSR, Indore is gratefully acknowledged.

REFERENCES

[1] C.T. Black, C.B. Murray, R.L. Sandstrom, S. Sun, Science 290 (2000) 1131.
[2] C. Zhou, T.C. Schulthess, D.P. Landau, J. Appl. Phys. 99 (2006) 08H906.
[3] Young-Yeal Song N Mo and Patton C E 2005 J. Appl. Phys. 97 093901.
[4] Lee S, Drwiega J, Mazysk D, Wu Ch and Sigmund W M 2006 J. Mater. Chem. Phys. 96 2.
[5] J. L Gunjakar, A. M. More, V. R. Shinde, C. D. Lokhande, J. Alloy and Compounds, 465, 468 (2008).
[6] C.N. Chinnasamy, A. Narayanasamy, N. Ponpandian, K. Chattopadhayay, K.Shinoda, B. Jeyadevan, K. Tohji, K. Nakatsuka, T. Furubayashi, I. Nakatani, Phys.Rev. B 63 (2001) 184108-1–184108-6.
[7] R. Vestal, J.Z. Zhang, Int. J. Nanotechnol 1, 240–263 (2004).
[8] D.J. Fatemi, V.G. Harris, M.X. Chen, S.K. Malik, W.B. Ye, J. Appl. Phys. 85, 5172–5174 (1999).
[9] N. Sivakumar, A. Narayanasamy, N. Ponpandianb, J. Appl. Phys. 101, 084116-1–084116-6 (2007).
[10]M. A. Amer, M . EI Hiti, Journal of Magnetism and Magnetic Materials 234 (2001) 118.
[11]Rodríguez-Carvajal, Physica, B, 192, 55-69(1993).
[12]G. Dixit, J.P. Singh, R.C. Srivastava, H. M. Agrawal, R. J. Choudhary, Adv. Mat. Lett. 3, 21-28(2012).
[13]J. Smit, H.P.J. Wijn, Ferrites, John Wiley, New York, 1959.
[14]J. Kreisel, G. Lucazeau, H. Vincent, J. Solid State Chem. 137, 127–137 (1998).
[15]J. Kreisel, G. Lucazeau, H. Vincent, J. Solid State Chem. 137, 127–137 (1998).
[16]B. Cui, H. Lin, Y.-Z. Liu, J.-B. Li, P. Sun, X.-C. Zhao, C.-J. Liu, J. Phys. Chem. C 113, 14083-14087 (2009).
[17]L. Hu, L. Wu, M.Y. Liao, X. Hu, X.S. Fang, Adv. Funct. Mater. 22, 998-1004 (2012).